Science Signaling
AAAS

www.sciencesignaling.org/cgi/content/full/6/288/ra69/DC1

Supplementary Materials for

A Computational Model Predicts That Gβγ Acts at a Cleft Between Channel Subunits to Activate GIRK1 Channels

Rahul Mahajan, Junghoon Ha, Miao Zhang, Takeharu Kawano, Tohru Kozasa, Diomedes E. Logothetis*

*Corresponding author. E-mail: delogothetis@vcu.edu

Published 13 August 2013, *Sci. Signal.* **6**, ra69 (2013)
DOI: 10.1126/scisignal.2004075

This PDF file includes:

Other Supplementary Material for this manuscript includes the following:
(available at www.sciencesignaling.org/cgi/content/full/6/288/ra69/DC1)

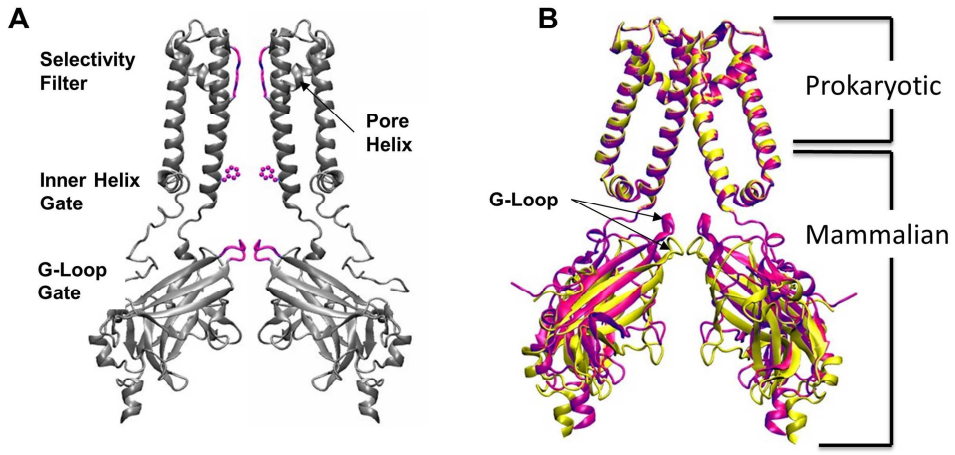

Fig. S 1. Permeation pathway, gates, and closed and open crystal forms of the intracellular G loop gate of a GIRK1 chimera. (**A**) Cartoon depiction of two opposite subunits of the GIRK1 chimera channel, composed of prokaryotic and mammalian portions as indicated in B. Putative gates along the potassium permeation pathway are highlighted in magenta and labeled on the left. (**B**) Overlapping cartoon depiction of the two crystallized conformations depicting the G loop gate in the constricted or "closed" (yellow) and the dilated or "open" (magenta) conformations.

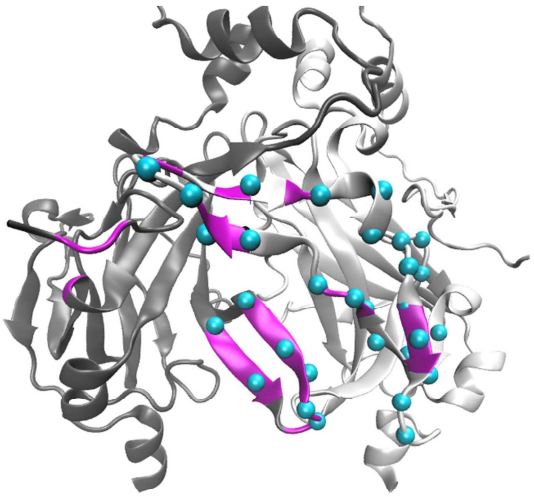

Fig. S 2. Comparison of our best-scoring computational model with an NMR model of the footprint of Gβγ on GIRK1 residues. The cartoon depicts the cytosolic domains of the channel and only two adjacent channel subunits are shown for clarity. Cyan spheres highlight the channel residues implicated in the Gβγ binding site (5Å cutoff) by our model. Magenta highlights depict the GIRK1 residues that interact with Gβγ identified in the NMR study of Yokogawa *et al*. (*32*).

Best Scoring Model:

Gβγ	:	Channel
ARG52	:	GLU334 GLU335
GLY53	:	SER332 LEU333 GLU334
LEU55	:	SER332 LEU333 SER235 PHE243 PRO245
ASP76	:	GLN237 PHE243
GLY77	:	PHE243
LYS78	:	PRO329 ILE331 SER332 PHE243 PRO245
N88	:	K339
LYS89	:	SER332 GLU334 LYS339 ASP341 SER343 GLN344
VAL90	:	SER343 GLN344
HIS91	:	PHE328 SER343 GLN344 ALA347
ALA92	:	PHE328 PRO329 ASP341 GLN344
ILE93	:	PHE328 PRO329 GLN344 PHE349
PRO94	:	ARG326 PHE327 PHE328 PRO329 PHE349 GLY241 GLU242 PHE243
LEU95	:	ARG326 PHE349 GLY241 PHE243
ARG96	:	ARG326 PHE349 GLU350 VAL351 PRO352 GLU240 GLY241
SER98	:	PHE243
TYR124	:	PHE328 PHE349 GLU350
GLU130	:	GLU198 HIS199 LEU322
GLY131	:	ALA347
ASN132	:	HIS199 LEU322 HIS325 HIS346 ALA347 THR348 PHE349
VAL133	:	PHE328 GLN344 ALA347 THR348 PHE349 GLU350
ARG134	:	LEU322 HIS325 PHE328 THR348 PHE349 GLU350
VAL135	:	PHE349 GLU350 VAL351

Largest Cluster Model:

Gβγ	:	Channel
ARG52	:	GLU334 GLU335
GLY53	:	SER332 GLU334
HIS54	:	LEU333
LEU55	:	PHE243 PRO245 PRO329 VAL330 ILE331 SER332 LEU333
ALA56	:	PHE243
LYS57	:	GLN237 PHE243
TYR59	:	GLN237
GLN75	:	GLN237 GLY241 PHE243
ASP76	:	PHE243 PRO329
GLY77	:	PHE328
LYS78	:	PHE328 PRO329 VAL330 ASP341 GLN344
ALA92	:	GLN344
PRO94	:	PHE328 GLN344
LEU95	:	PHE328 PHE349 GLU350
ARG96	:	PHE349 GLU350 VAL351 PRO352
SER97	:	PHE349 GLU350 VAL351 PRO352
SER98	:	GLU240 GLY241 GLU242 PHE243 ARG326 PHE349 VAL351 PRO352
TRP99	:	GLN237 THR238 PRO239 GLU240 GLY241
SER334	:	LEU333
PHE335	:	LEU333

Fig. S 3. Gβ- and GIRK1-interacting residues in the best-scoring and largest cluster models. Predicted interactions (5Å cutoff) for our best-scoring (left) and largest cluster (right) models. No interactions with Gγ are predicted, all listed residues refer to Gβ. Residue numbering is according to human GIRK1 protein and bovine, which is identical in amino acid sequence to human, Gβ1.

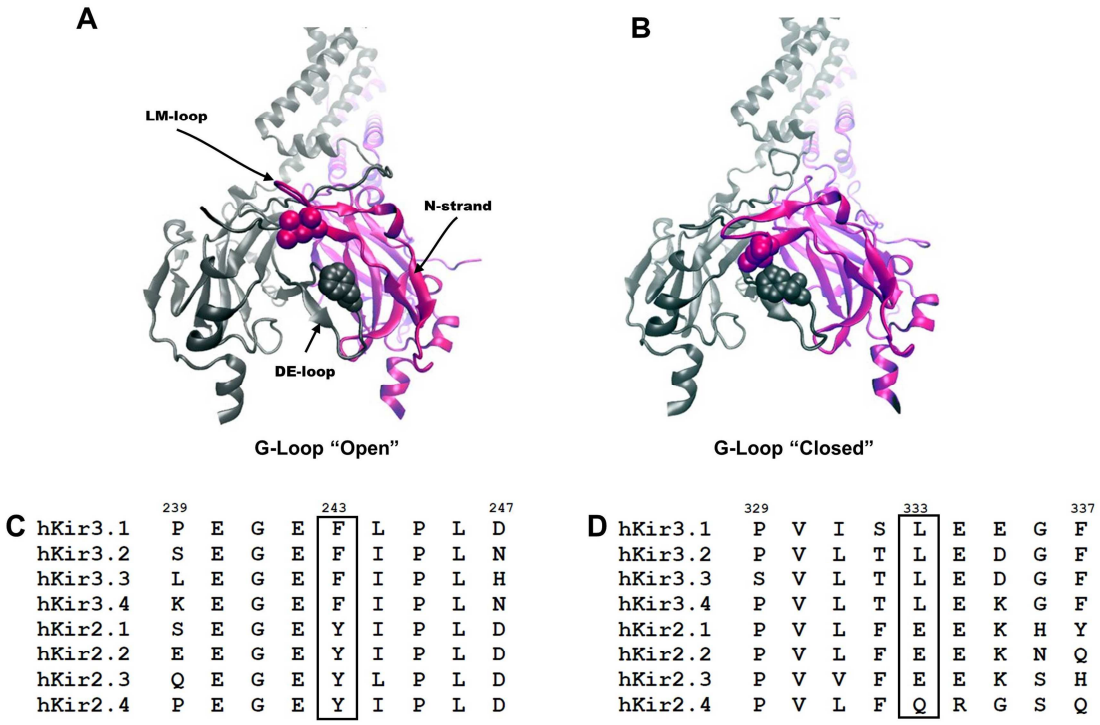

Fig. S 4 . Critical elements of the open versus closed G loop conformations of the channel structure. (**A**) Cartoon depiction of two adjacent subunits (magenta and gray) of the "open" G loop conformation of the channel structure. The LM loop residue Leu^{333} (magenta) and the DE loop residue Phe^{243} (gray) are highlighted as spheres on two adjacent subunits. A cleft is visible separating the two residues. (**B)** Cartoon depiction of two adjacent subunits (magenta and gray) of the "closed" G loop conformation. The cleft between Leu^{333} (magenta) and the Phe^{243} (gray) is occluded and the residues are close together. (**C**) Differential conservation of GIRK1(F243). Phe^{243} is absolutely conserved in all human GIRK (Kir3.x) isoforms. In IRK (Kir 2.x) channels, this position is occupied by a conserved Tyr rather than a Phe residue. (**D**) Differential conservation of GIRK1(L333). Leu^{333} is fully conserved in all human GIRK isoforms, but in IRK channels it is changed to a charged or polar residue.

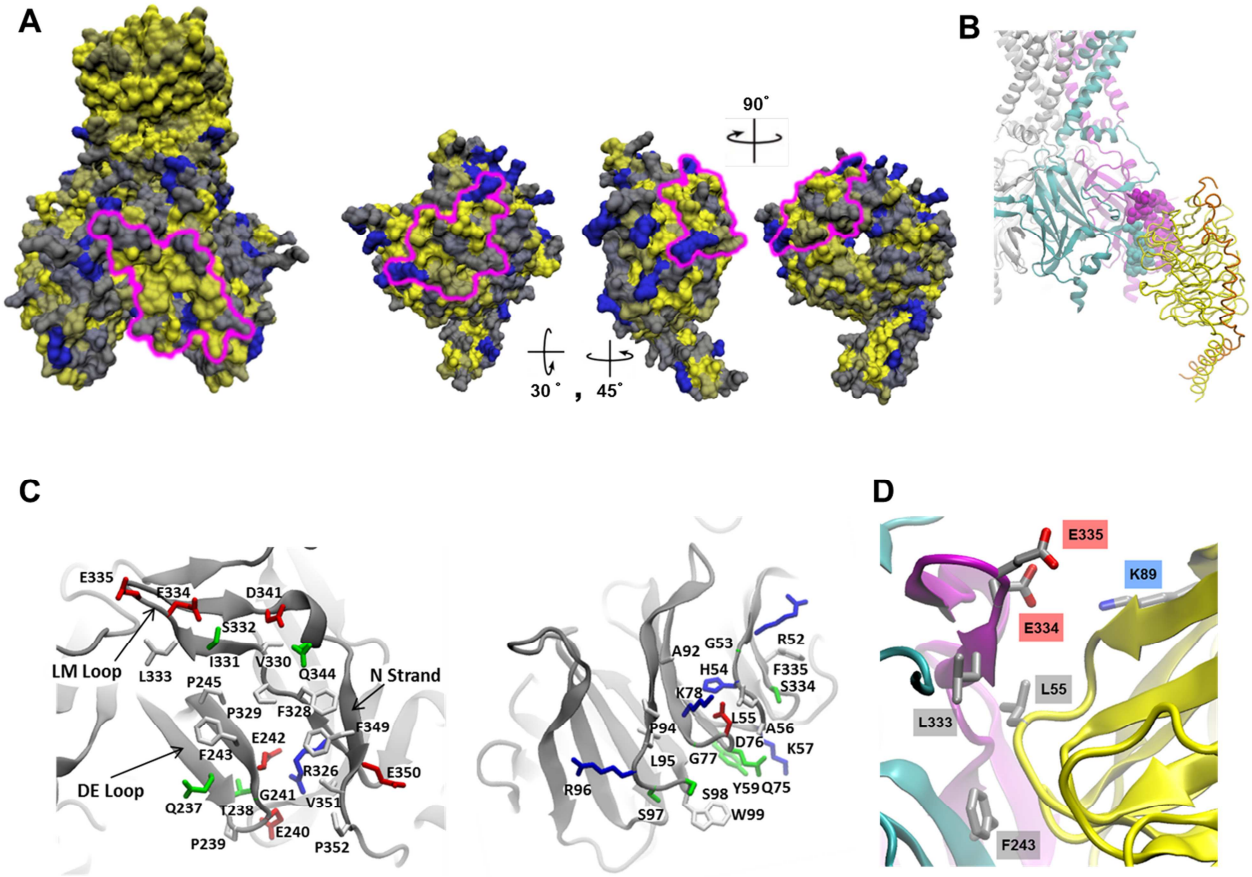

Fig. S5. Largest cluster model details. (**A**) Surface representations of the channel (left) and Gβγ (right) are colored by residue hydrophobicity *(44)*: Yellow is most hydrophobic, blue is least hydrophobic. Interface regions found in the largest cluster model are outlined in magenta. (**B**) Cartoon illustration showing overall orientation of Gβγ docked to the channel. Gβ is yellow (ribbon), Gγ is orange (ribbon), two adjacent subunits of the homotetrameric channel are highlighted in cyan and magenta (cartoons). Interface residues of the channel subunits within 5Å of Gβ are depicted as spheres. (**C**) Close-up views depicting cartoon backbone and stick sidechain representations of interface residues (5Å cutoff) of the channel (left) and Gβγ (right). In C, red = acidic, blue = basic, green = polar, white = non-polar. (**D**) Cartoon illustration of predicted functionally important residue interactions. Two adjacent subunits of the channel are highlighted in cyan and magenta. Gβ is yellow. Gβ Leu^{55} is seen inserting in a cleft between GIRK1 LM loop residue Leu^{333} and DE loop residue Phe^{243} of adjacent channel subunits. GIRK1 residues Glu^{334} and Glu^{335} are also seen near Gβ Leu^{55} and Lys^{89}. Residue numbers are shaded as gray, hydrophobic; blue, positively charged; red, negatively charged.

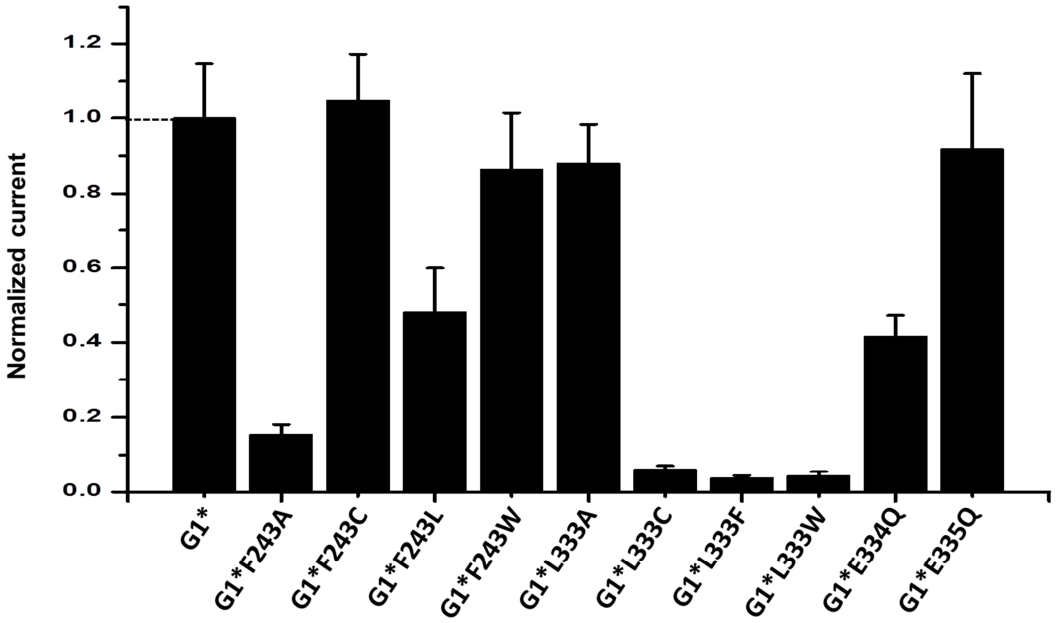

Fig. S 6. Effect of channel mutations on mean currents relative to the G1*. Current amplitudes relative to the control G1*. One way ANOVA with Dunnett's post hoc test demonstrated that none of the mean currents for any of the channel mutants was significantly greater than that of G1*.